ASEAN Engineering Journal

Full Paper

NONLINEAR SIMULATIONS TO EVALUATE THE CODE-BASED RESPONSE MODIFICATION FACTOR FOR SEISMIC DESIGN OF SLAB-ON-PILE STRUCTURE

Muhamad Fauzi Darmawan, Angga Fajar Setiawan*, Iman Satyarno, Ali Awaludin

Department of Civil and Environmental Engineering, Universitas Gadjah Mada, Yogyakarta, Indonesia

Article history
Received
04 April 2023
Received in revised form
28 July 2023
Accepted
14 August 2023
Published online
29 February 2024

*Corresponding author
angga.fajar.s@ugm.ac.id

Graphical abstract

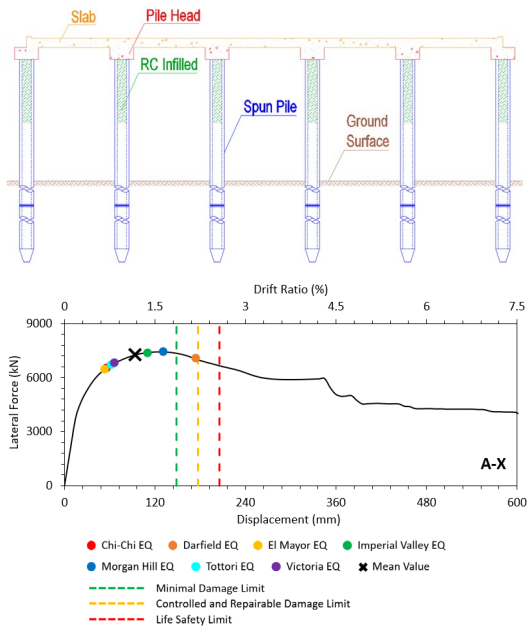

Abstract

Slab on Pile (SOP) structure using concrete spun pile (CSP) is frequently constructed for highway or railway infrastructures in Indonesia. However, some previous studies showed that spun piles have low energy dissipation and ductility. Therefore, spun pile application as bridge piers, particularly in high seismic locations such as Indonesia, needs additional consideration. The response modification factor (*R*) in the SOP elastic seismic design needs to be carefully considered since this parameter reflects the ability of the structure to dissipate energy through inelastic behavior. The work discussed in this paper primarily concerns the evaluation of the *R*-value based on the Indonesia seismic bridge design code, SNI 2833-2016, which is applied to SOP seismic design. The study provided an alternative reference for engineers in the seismic design of a SOP structure. Preliminary elastic design of SOP structures demonstrated that the number of piles and structural flexibility is significantly affected by the *R*-values consideration. In addition, the pinching hysteresis captured from the nonlinear dynamic analysis results emphasized the limited capability of an SOP structure in dissipating energy under seismic excitation. Moreover, the spun pile concrete material, especially in the pile-to-pile head connection, was observed to have an earlier failure. This study strongly suggested using an R-value of 1.5 to achieve a high seismic performance SOP structure with little need for aftershock retrofitting, even though this would necessitate much more spun piles. However, some further research could be conducted to develop the high seismic performance but economical design of SOP structures.

Keywords: SOP structure, spun pile, response modification factor, performance-based evaluation, nonlinear analysis

1.0 INTRODUCTION

Slab on Pile (SOP) is an elevated structure widely constructed for highway or railway infrastructures in Indonesia. The structure contains piles, pile heads, and concrete slabs. Figure 1 shows an example of an SOP structure application in the railway infrastructure of Indonesia. Faster and lower-cost construction are some advantages of choosing an SOP structure. In addition, the SOP structure effectively overcomes the low bearing capacity and significant settlement problems of highway structures constructed in a peat soil zone [1].

Concrete spun pile (CSP) is commonly used for SOP structure construction in Indonesia due to the efficient construction cost and time. Moreover, spun pile relatively has controlled and consistent quality from the off-site fabrication [2]. However, the spun pile has low energy dissipation and ductility [2], [3]. Setiawan et al. [4] reported that the equal damping ratio generated by the spun pile was below 10%. In addition, spun pile shows a brittle failure mechanism due to the fracture of the prestressing tendon [3]. Due to the prestressing effect, the axial force increases the pile capacity carrying gravity loads but drops the structure's ductility [5]. Therefore, spun pile application as bridge piers, especially in the high seismic region, needs more attention.

Figure 1 Application of SOP structure in Adi Soemarmo Airport Railway, Indonesia.

Considering Indonesia generally has high seismic risk and hazard, the SOP structure must be designed to withstand earthquakes. The seismic design of the SOP structure in Indonesia is based on SNI 2833:2016, the Indonesia seismic design code for the bridge structure. This code adopted the AASHTO LRFD Bridge Design Specification. The seismic design force is developed using a force-based design method for the yielding elements by introducing a response modification factor (*R*). The *R*-value reduces the elastic seismic force calculated from the demand analysis to the inelastic one [6]. It represents the capability of a structure to dissipate energy through inelastic behavior [7].

Some studies or design practices of SOP structure in Indonesia applied the response modification factor provided by SNI 2833:2016, considering the spun piles as multi-column bent and a particular bridge operational category. For instance, Jasin (2018) implemented an *R*-value of 5 following the ordinary bridge operational category [8]. An *R*-value of 3.5 was considered by Putri and Purwanto (2018) following the essential bridge operational category [9]. Furthermore, since SOP has a similar structural configuration to the wharves structure, which utilizes extended piles to support the main slab, ASCE 61-14 was worth referring to. ASCE 61-14 specified using *R*=2 for the wharf structure's seismic design using a prestressed concrete pile with a connection system that meets the code requirement [10]. This requirement was followed by Belani et al. (2021) to analyze a wharf structure in Nabire, Indonesia [11].

Nonlinear simulations, both static pushover and dynamic response history analysis, were widely used to evaluate the seismic performance of the wharves structure [12]–[17]. However, limited study has been conducted on seismic performance evaluation of SOP structures as highway or railway viaduct using nonlinear simulation. Pushover analysis was used by Oktavina et al. (2022) to evaluate the SOP structure considering the *R*-value of 3 [18]. A previous study by Darmawan (2022) and Haroki (2023) compared the seismic performance of two types of spun pile-supported bridge structures, which were preliminary designed considering *R*-values of 1.5 and 3.5 [19] and [20]. Furthermore, the addition of a shear panel damper was proposed. However, reinforced concrete (RC) infilled in the pile-to-pile head connection was still neglected. The structure with an *R*-value of 3.5 required about two times fewer spun piles to satisfy the code. Nevertheless, the nonlinear analysis using both pushover and time history analysis showed that the SOP seismic response demands exceeded the life safety performance limit. However, the seismic device equipment could enhance the structural performance of SOP with the R-value of 3.5 below the minimal damage level.

The work presented in this paper focuses on evaluating response modification factors based on SNI 2833:2016 applied for the seismic design of SOP structures. Three types of SOP structures were designed using different response modification factors provided by the code. Reinforced concrete infilled in the spun pile was considered following the actual construction method of the SOP structure. Nonlinear pushover and time history analysis were then conducted to capture the structural behavior and performance of the three different SOP structures under seismic excitations.

2.0 METHODOLOGY

2.1 Structural Configuration and Seismic Design of SOP Structure

Three types of SOP structures were preliminary designed as an elevated double-track railway. Response modification factors of 1.5, 3.5, and 5.0 were applied for SOP A, B, and C, respectively. The design focused on determining the number of spun piles that satisfied the Indonesian bridge seismic design provision, considering the piles as multi-column bents. Meanwhile, the pile head and slab element were not designed in detail here. Figure 2 shows the typical configuration of a single SOP structure segment considered in this study. A segment with a total of 20 m length was considered in this study. The SOP structure had free-standing piles above the ground and embedded pile of 5 meters and 30 meters in length, respectively. Meanwhile, Figure 3 describes the spun pile element and concrete plug detail. Each pile was divided into two zones. Zone A combined the spun pile and concrete plug. This zone was 2.5 m long from the top of the pile, while the remaining was Zone B, which was the spun pile section only.

The compressive strength (f'_c) of the spun pile concrete was 54.4 MPa. The spun pile had 24 prestressed concrete (PC) bars with a diameter of 9.2 mm. The elastic modulus of the PC bar was 220,267 MPa. The yield and ultimate stresses of the PC bar were 1,387 MPa and 1,455 MPa, respectively, following Irawan et al. (2018). The PC bars were subjected to 5,000 με initial tensile strain [21]. Meanwhile, for the other components, i.e., pile head, slab, and concrete plug, the compressive strength is 25 MPa. The reinforcement steel bar had yield and ultimate stresses of 420 MPa and 520 MPa, respectively.

SAP2000 was utilized to develop the numerical model of the SOP structures in the preliminary design phase, as shown in Figure 4. The pile and pile head were modeled using a frame element, while the slab was modeled using a thick shell element. The fix-based approach was implemented in the structural model. The piles were assumed to be fixed at 3 meters below the ground surface, as shown in Figure 3, based on the calculation shown in Table 1 following [22] as specified in AASHTO LRFD Bridge Specification.

The seismic design was based on axial-moment interaction from all pile elements compared to the diagram interaction of the pile sections. The internal forces of the spun pile were obtained with the category of Strength I and Extreme I load combinations specified by the code. The loads consisted of dead load (MS), additional dead loads (MA), live load (LL), and earthquake effect (EQ). The dead load was self-weight of the SOP structures, including spun pile, pile head, and slab. SAP2000 automatically counted these loads. The additional dead loads

comprised the parapet, ballast, concrete sleepers, and steel rail. Meanwhile, the live load was the trains passing over the structure.

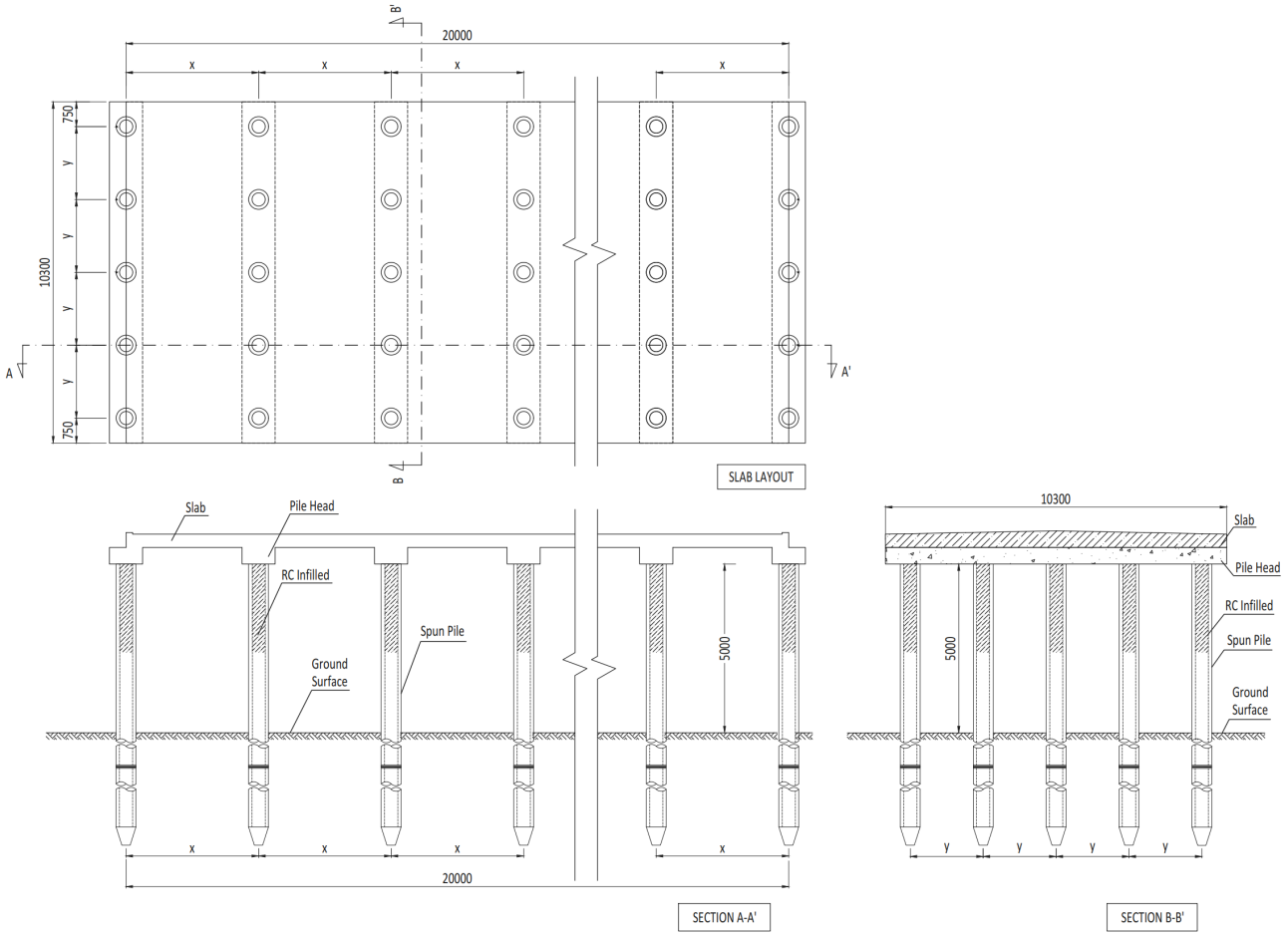

Figure 2 Typical configuration of a single SOP structure segment (unit in mm)

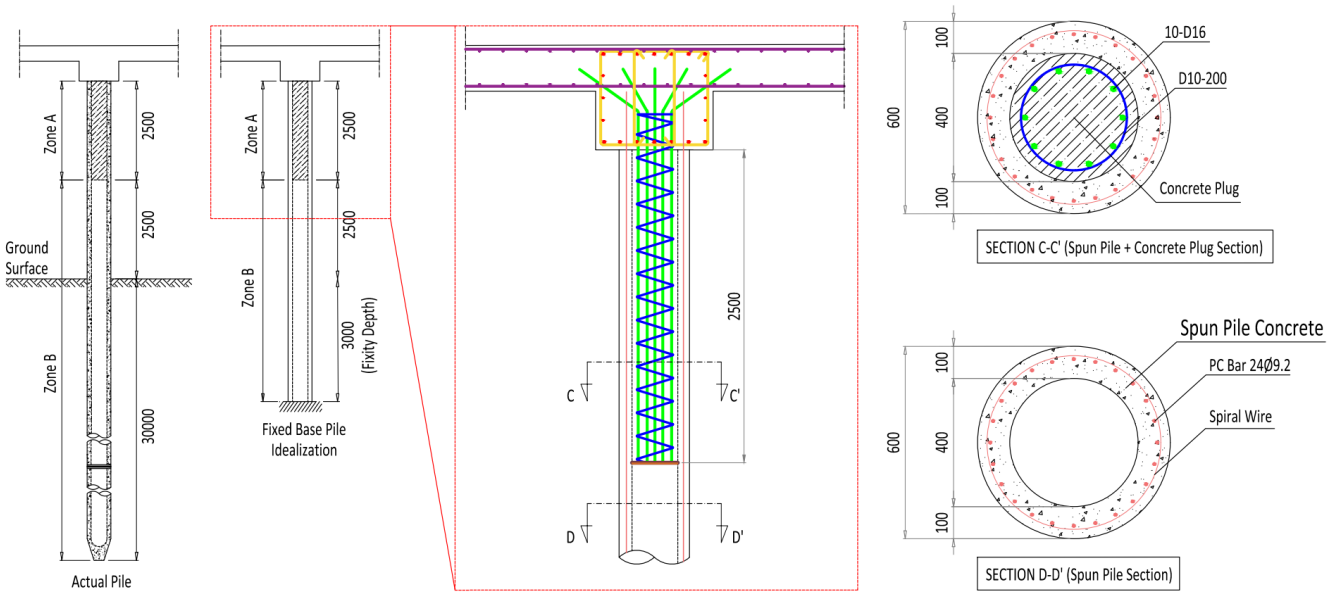

Figure 3 Detail of spun pile element and concrete plug (unit in mm)

Table 1 Fixity depth of the pile after Davisson and Robinson (1965); Darmawan (2022).

Compressive strength of concrete,	$f_c' =$	54,4	MPa
Modulus elasticity of the pile material,	$E = 4700 * \sqrt{f'_c} =$	34665,49	MPa
Moment inertia for pile section,	$I =$	5345090000	mm^4
Rate of increase of soil modulus,	$n_h =$	0,013	MPa/mm
Stiffnes factor,	$T = (E*I/n_h)^{0.2} =$	1701,30	mm
Fixity depth,	$z_f = 1.8*T =$	3062,35	mm

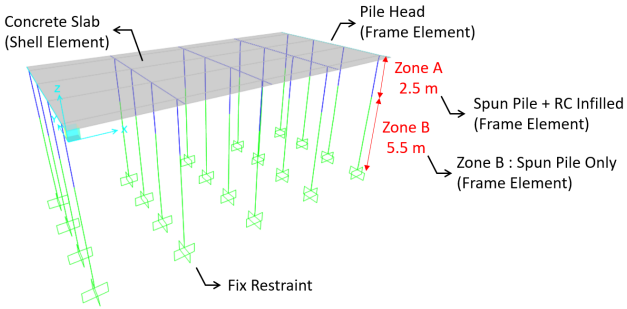

Figure 4 Fixed base numerical model of an SOP structure developed using SAP2000.

The earthquake effect was considered using response spectrum analysis. The design spectrum was generated based on SNI 2833:2016 [23]. The structure was considered to be located in Yogyakarta Province, Indonesia. The short period (S_s), one-second period (S_1) and peak ground acceleration (PGA) parameters for the considered location were 0.9 g, 0.4 g, and 0.4 g, respectively, according to Indonesia seismic zone maps for a probability of exceedance 7% in 75 years provided by the code. Site classification was determined based on the soil profile's average Standard Penetration (SPT). Based on a given bor-log data as shown in Figure 5, the average $\bar{N}$ (number of penetration) was calculated. Since $\bar{N} < 15$, then the site shall be classified as Site Class E. Based on the S_s & S_1 stated before and Site Class E, the site coefficients were obtained, i.e., $F_{PGA} = 0.9\,g$, $F_a = 1.02\,g$, and $F_v = 2.4\,g$. The spectral design response parameters were then calculated, i.e., $A_s = 0.36\,g$, $S_{DS} = 0.918\,g$, and $S_{D1} = 0.96\,g$. The design spectrum is depicted in Figure 6. Since $S_{D1} > 0.5$, the SOP structure was assigned to Seismic Zone 4.

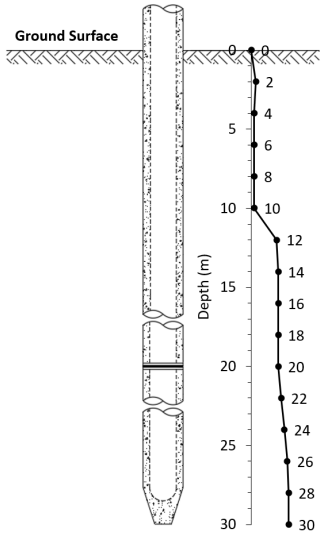

Figure 5. Bor log (SPT value) of soil profile at problem site

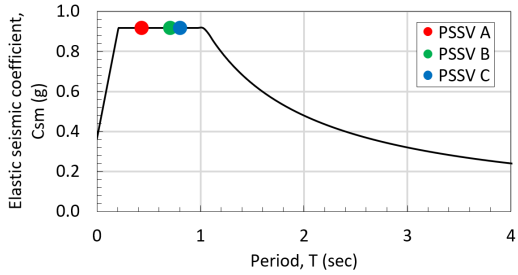

Figure 6 Design spectra based on SNI 2833:2016 (modified from [6])

2.2 Ground Motion Modification

This study modeled a set of synthetic ground motions to perform nonlinear time history analysis for the SOP structures. Seven pairs of ground motion time histories were selected as recommended by SNI 2833:2016. The initial screening of ground motions was based on the source mechanism, magnitude, site soil condition, site-to-source distance, and spectral shape, as explained in [24]. The selected seed motions were shallow crustal earthquakes with strike-slip mechanisms since the Opak fault is near the structure. The magnitude and source-to-site distance of the seed motion were based on the de-aggregation result for Yogyakarta by Sunardi [25]. The amplitude scaling method adopting SNI 8899:2020 [26] was used to modify the seed motions. Figure 6 demonstrates that the scaling had fulfilled the requirement to ensure the average spectrum above the 90% target spectrum within the period range of interest. The final scaled ground motions used for performing the NLTH analysis can be seen in Figure 8.

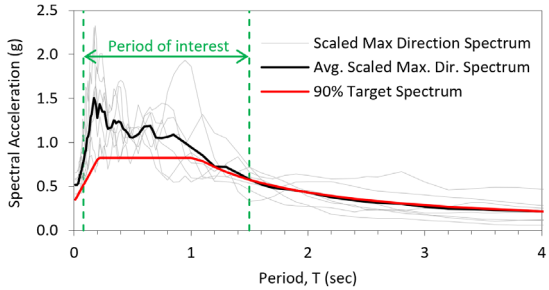

Figure 7. Comparison between the scaled maximum direction spectrum and the target spectrum (modified from [6]).

2.3 Structural Performance Limit

An SOP structure is typically similar to a pier and wharf structure. Therefore, the performance level to evaluate the SOP structures' performance in this study was based on ASCE 61-14. There are three performance levels. The first level is Life Safety Protection (LSP) which marks that the structure under severe earthquake continues to support gravity loads without damage preventing egress. Controlled and Repairable Damage (CRD) is the second level, which indicates that the structure responds in a controlled and ductile behavior, with restricted inelastic deformations at repairable locations. In addition, the required repairs result in a period of loss of serviceability for no more than a few months. The last level is Minimal Damage (MD). A structure suffers "minimal damage" when it demonstrates near-elastic structural response with minimum or no residual deformation and no loss of serviceability. No loss of material containment is allowed at all levels that would pose a public safety risk [10].

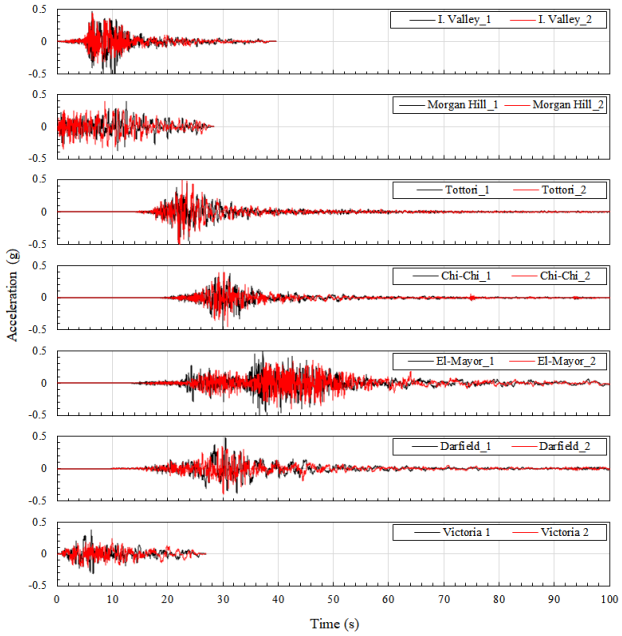

Figure 8 Synthetic ground motions for NLTH analysis of the SOP structures (modified from [6])

The structural performance was determined by monitoring the strain of the materials constructed in the piles when the structure experienced both gravity and lateral loads. Table 2 summarizes the strain limits corresponding to the structural performances according to ASCE 61-14.

Table 2 Structural Performance Level Limits based on ASCE 61-14 [10]

Performance Level	Component	Strain Limit
Minimal Damage	Concrete	$\varepsilon_c \leq 0.004$
	Reinforcing Steel	$\varepsilon_s \leq 0.015$
	Prestressing Steel	$\varepsilon_s \leq 0.015$
Controlled and Repairable Damage	Concrete	$\varepsilon_c \leq 0.006$
	Reinforcing Steel	$\varepsilon_s \leq 0.040$
	Prestressing Steel	$\varepsilon_s \leq 0.020$
Life Safety Protection	Concrete	$\varepsilon_c \leq 0.008$
	Reinforcing Steel	$\varepsilon_s \leq 0.060$
	Prestressing Steel	$\varepsilon_s \leq 0.025$

2.4 Nonlinear analysis using OpenSees

Nonlinear static pushover and time history analysis were carried out to evaluate the structural performance of the SOP structures in this study. The analyses were performed using OpenSees [27] since it can simulate the nonlinear behavior of spun pile element better than SAP2000 [6]. In addition, STKO software was utilized to do the pre and post-processing of the analyses [28]. Figure 9 depicts a sample model of an SOP structure developed using STKO. Since the fix-based approach was considered, all bottom nodes of the piles were fixed in all degrees of freedom. The dead, additional dead, and live loads were assigned as distributed frame loads. In addition, the pushover lateral load was assigned in all top pile nodes.

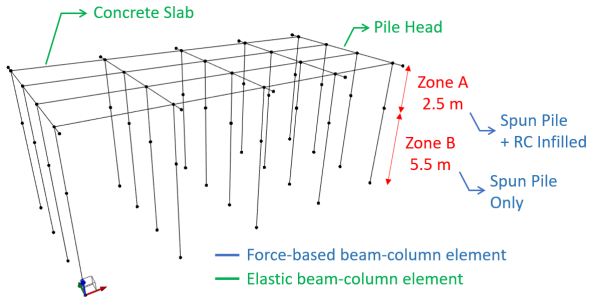

Figure 9 SOP structure model in STKO

The spun pile was modeled using a force-based beam-column element considering the P-Delta effect. Gauss-Lobatto integration method with three integration points was implemented in the spun pile element. Concrete02 was used to define the stress-strain curve for concrete. Steel01 and Reinforcing Steel material were utilized to define the prestressing and reinforcing steel material, respectively. MinMax material was implemented for Steel01 material to limit the strain of both prestressing and reinforcing steel material. If the strain exceeds the specified threshold values, i.e., the ultimate strain of the steel material, the other material is assumed to have failed. In addition, the initial strain material was implemented for prestressing steel material to apply the initial prestressing effect. Figure 10 shows the stress-strain relationship of materials used in the spun pile section. Meanwhile, the pile head and the slab elements were constructed as elastic beam-column elements assuming that these elements remain within the elastic behavior.

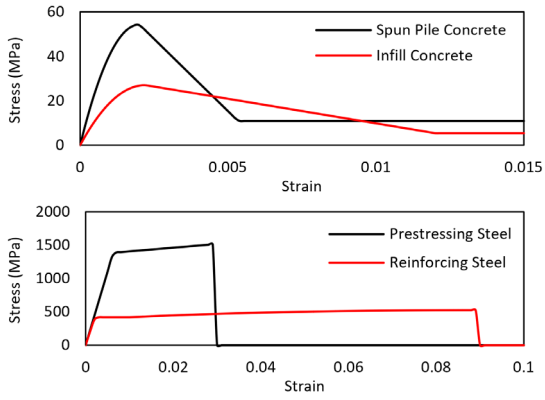

Figure 10 Stress-strain relationship of concrete and steel material used in the spun pile section

3.0 RESULTS AND DISCUSSION

3.1 Seismic Design Result

According to the abovementioned design method, pile elements' internal force responses (axial-moment interaction and shear force) were examined to determine the number of piles needed for each SOP structure. Table 3 summarizes the preliminary seismic design result of the SOP structures, which satisfied SNI 2833:2016. It was clear that response modification response significantly affects the number of piles in an SOP structure. The required number of spun piles is inversely related

to the *R*-value. The applied seismic force increases with decreasing *R*-value, increasing the need for more piles. SOP A required the greatest number of piles since a nearly elastic design approach was applied, compared to SOP A, SOP B, and SOP C needed 2.7 and 3.6 times fewer piles, respectively.

Table 3 Parameter of the designed SOP structures

SOP	*R*-Value	Number of Bents	Piles in Each Bent	Total Piles	x (mm)	y (mm)
A	1.5	9	6	54	2500	1760
B	3.5	5	4	20	5000	2900
C	5	5	3	15	5000	4350

As previously mentioned, the number of piles in the SOP structure is proportional to the magnitude of the seismic force. It is accompanied by slightly similar moment forces on spun pile element of the three different SOP structures, as shown in Figure 11. The scatters on the other side draw that an SOP structure designed using a higher *R*-value experiences higher axial forces in the pile elements since the same total gravity loads were supported by fewer spun piles.

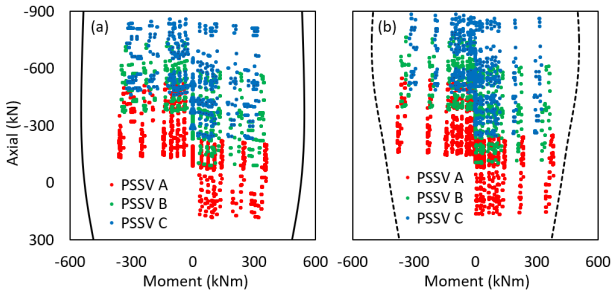

Figure 11 Axial force and moment response at pile elements compared to the interaction diagram of (a) Zone A and (b) Zone B sections

3.2 Structural Behavior

Table 4 summarizes the fundamental period of the SOP structures obtained from the modal analysis. It can be seen that all SOP structures had lower stiffness in the longitudinal direction rather than the transversal one. Moreover, the result shows that SOP A had the highest stiffness since it had the greatest number of piles. However, all of the SOP structures had a maximum value of spectral response acceleration corresponding to the natural period, as shown in Figure 6. It illustrates that the different response modification factor employed in the SOP structural design has no appreciable impact on the seismic acceleration the SOP structure is likely to experience.

The responses of all SOP structures under seismic excitation captured from nonlinear history analysis are shown in Figure 13. Lateral force refers to the base reaction of the structure. Meanwhile, displacement was observed in the top elevation of the pile. Pinching hysteresis curves are observed clearly in SOP A responses. It confirms that SOP structures have a low capability to dissipate or absorb the energy generated by earthquakes, for example. Cyclic analysis of an SOP structure carried out in a previous study shows that SOP structures using spun piles had a significantly lower energy dissipation capability than an SOP structure using the circular reinforced concrete column as the piers [29]. It is reasonable, considering spun pile has low energy dissipation, as explained before [2, 3, 4].

Table 4 Fundamental period of the SOP structures

SOP	Fundamental Period (s)	
	Longitudinal Direction	Transversal Direction
A	0.43	0.41
B	0.71	0.67
C	0.81	0.78

Pinching behavior can still be seen from SOP B under Chi-Chi, El-Mayor, Imperial Valley, and Victoria Earthquake. Meanwhile, responses of SOP B to other earthquakes tend to be asymmetric. It likely occurred because SOP B experienced a large response from these earthquakes, measuring nearly 400 mm or equivalent to a drift ratio of 5%. Unfortunately, the SOP C hysteresis curve appeared to be more irregular. It was possibly due to an extremely large reaction of the SOP C under seismic excitations, which led to the structure's severe failure and destabilization.

3.3 Performance Limit

Strain responses in the fiber section of the spun pile element were monitored through the pushover analysis result. Figure 12 depicts the displacement level at which the strain exceeded the strain limit of the corresponding performance level, as presented in Table 2. Generally, there was no significant difference in results in both the longitudinal and transversal direction of the SOP structure. It was in line with the identical pushover curves between the two orientations, as shown in Figure 14.

Compared to other materials, it is noticeable that spun pile concrete material first attained the limits of all performance levels. For instance, the life safety protection limit of the spun pile material was exceeded when the drift ratio fell over 2.7%. Meanwhile, a larger drift ratio of up to 3.75% was required to achieve the life safety protection performance based on the prestressing steel strain. It indicates that when the SOP structure is subjected to lateral loads, such as an earthquake, the spun pile concrete material is the first to have a failure. It coincides with an experiment on cyclic loading of hollow prestressed piles by Benzoni et al. [2]. According to the study, concrete spalling caused the pile's failure mechanism to initiate.

Additionally, earlier spun pile concrete and prestressing steel failure in Zone A was captured. It showed that the connection between the spun pile and the pile head suffered greater force than the embedded pile. It was probably caused by the concrete plug's higher stiffness of Zone A. A nonlinear pushover analysis of an SOP structure carried out by Oktavina et al. [18] showed that most failures of the spun pile element also occurred at the connection with the pile head. To enhance the seismic performance of the SOP structure, careful design of the spun pile concrete is, therefore, necessary, particularly at the connection between the spun pile and the pile head.

The concrete plug on the other side could survive even if the SOP structure were severely displaced. Up to a drift ratio of 5%, the infill concrete's strain did not exceed the life safety protection limit. Moreover, the reinforcing steel material held up despite the drift ratio beyond 10%.

3.4 Structural Performance

The maximum response of SOP structures under seismic excitations obtained from nonlinear time history analysis was plotted in the skeleton curves of the SOP structures, as shown in Figure 14. The mean value of the maximum responses was provided as permitted by [23] to make observing the seismic performance of the SOP more straightforward. The charts also featured the lines representing the spun pile concrete performance level limit at Zone A since they controlled the structure's performance limit, as previously noted.

The SOP structures designed using a response modification value of 1.5 had the best seismic performance. SOP A could maintain the seismic performance below the minimal damage level. On the contrary, SOP C, designed using an R-value of 5, had the worst seismic performance. Under almost all earthquakes, the SOP C response exceeded the life safety limit. Meanwhile, SOP B performed better than SOP C. However, the longitudinal and transversal mean values of the SOP B responses were over and nearly at the life safety limit, respectively. According to the pushover analysis curve shown in Figure 14, even though the life safety limit is 2.0% to 2.7% of drift ratio, all SOP structural models showed gradual (stable) strength degradation after this. The study implemented a nonlinear frame element that only considers the 1D element as uniaxial material behavior (only considering axial stress in the longitudinal direction of the frame element). The material's stress of spun pile section in the radial direction that exhibited brittle failure could not be captured. Thereby, the real brittle failure of the spun pile did not visible in this numerical model. Thus, in this study, the uniaxial limit strain of spun pile section was adopted according to the ASCE 61-14 [10].

Since repair is relatively difficult to do, failure or damage in a spun pile's embedded section should be avoided. Figure 15 emphasizes the poor performance of SOP C, which could experience a total collapse of the SOP structure at the pile under the ground surface. Meanwhile, the embedded-pile element of SOP B ranged between CRD and LS limit. Severe damage at the embedded pile could still emerge, which needed a big effort to do some retrofitting to the pile. On the other hand, almost no pile damage in the embedded zone was captured in the SOP A structure. Except for the Darfield Earthquake, all seismic excitation scenarios resulted in a maximum SOP A response below the minimal damage limit of the embedded pile.

Based on the above performance comparison, SOP C did not give an adequate seismic performance. So, an *R*-value of 5 is not recommended for the seismic design of an SOP structure, in line with Oktavina et al. [18]. The mentioned study suggested an *R*-value of 3 instead, resulting in an SOP structure with performance below life safety levels and was safe under an earthquake with a 1000-year return period. However, it was close enough to SOP B's performance, so some severe damage under seismic load would probably occur following this study. Furthermore, SOP A gave the highest seismic performance without significant damage on the spun pile. Although significantly more spun piles are required, this study highly recommended implementing an *R*-value of 1.5 to obtain an earthquake-resistant SOP structure with minimal retrofitting effort after an earthquake.

The *R*-value of 1.5 used for the SOP structure based on SNI 2833-2016 was close enough to the *R*-value required by ASCE 61-14 for wharf structures ranging from 1 to 2. Nevertheless, improving seismic performance for SOP structures that use higher R-values could be the subject of future research. Investigating the adequate pile-to-pile head connection design may improve seismic performance for a more cost-effective SOP construction to obtain a more economical SOP structural design.

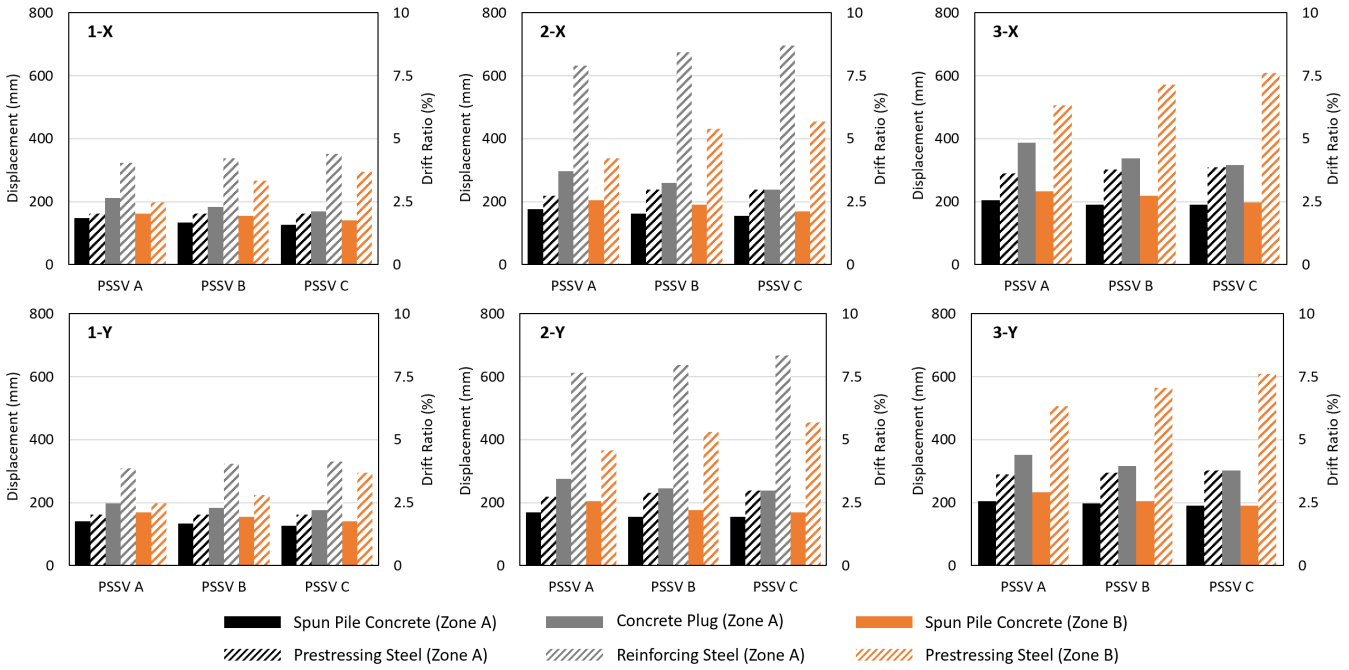

Figure 12 Displacement level at which the performance limit of SOP structures in both (X) longitudinal and (Y) transversal direction was exceeded: (1) Minimal damage, (2) Controlled and Repairable Damage, and (3) Life Safety Protection

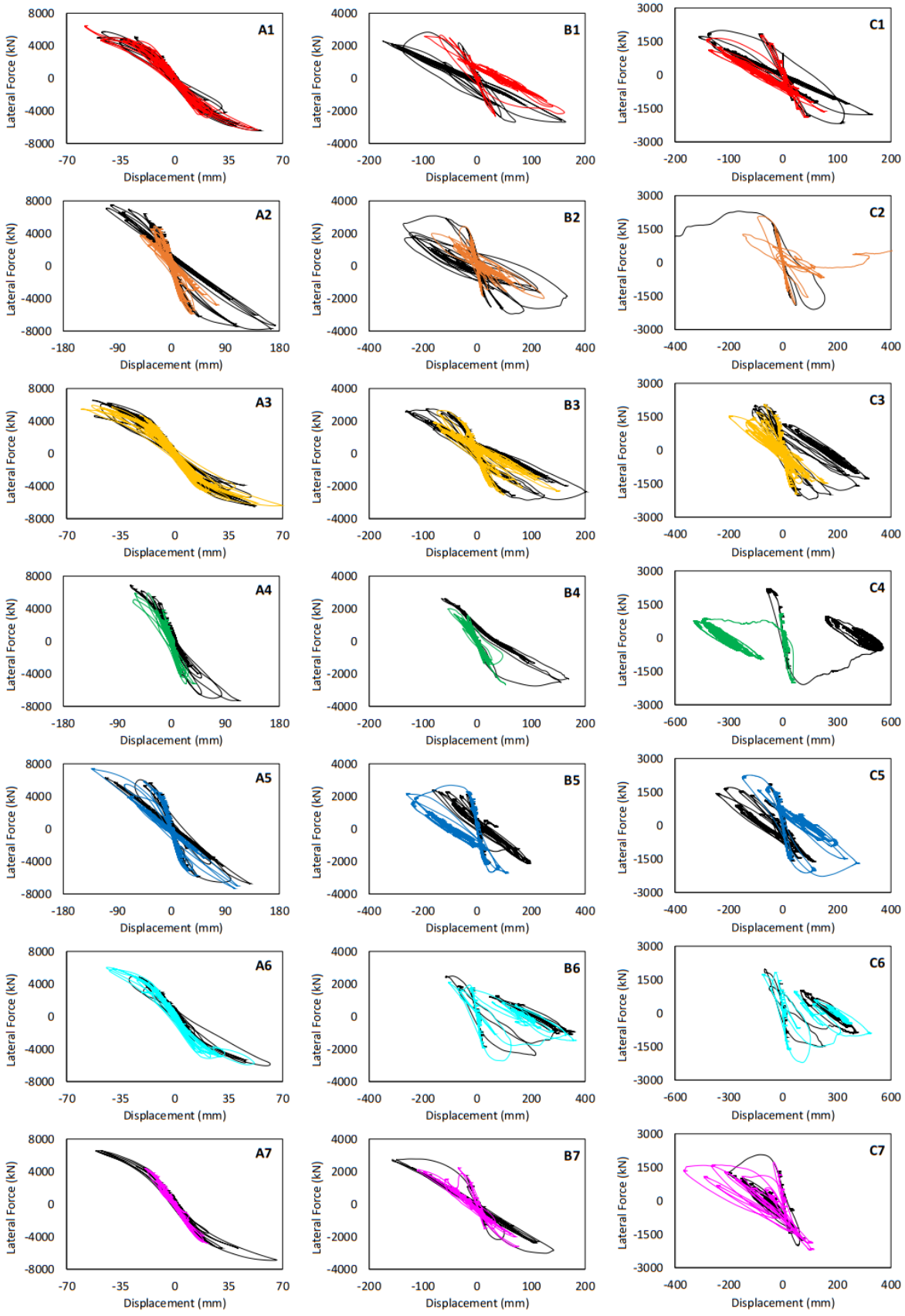

Figure 13. Seismic response history of (A) SOP A, (B) SOP B, and (C) SOP C structures under (1) Chi-Chi, (2) Darfield, (3) El-Mayor, (4) Imperial Valley, (5) Morgan Hill, (6) Tottori, and (7) Victoria Earthquakes

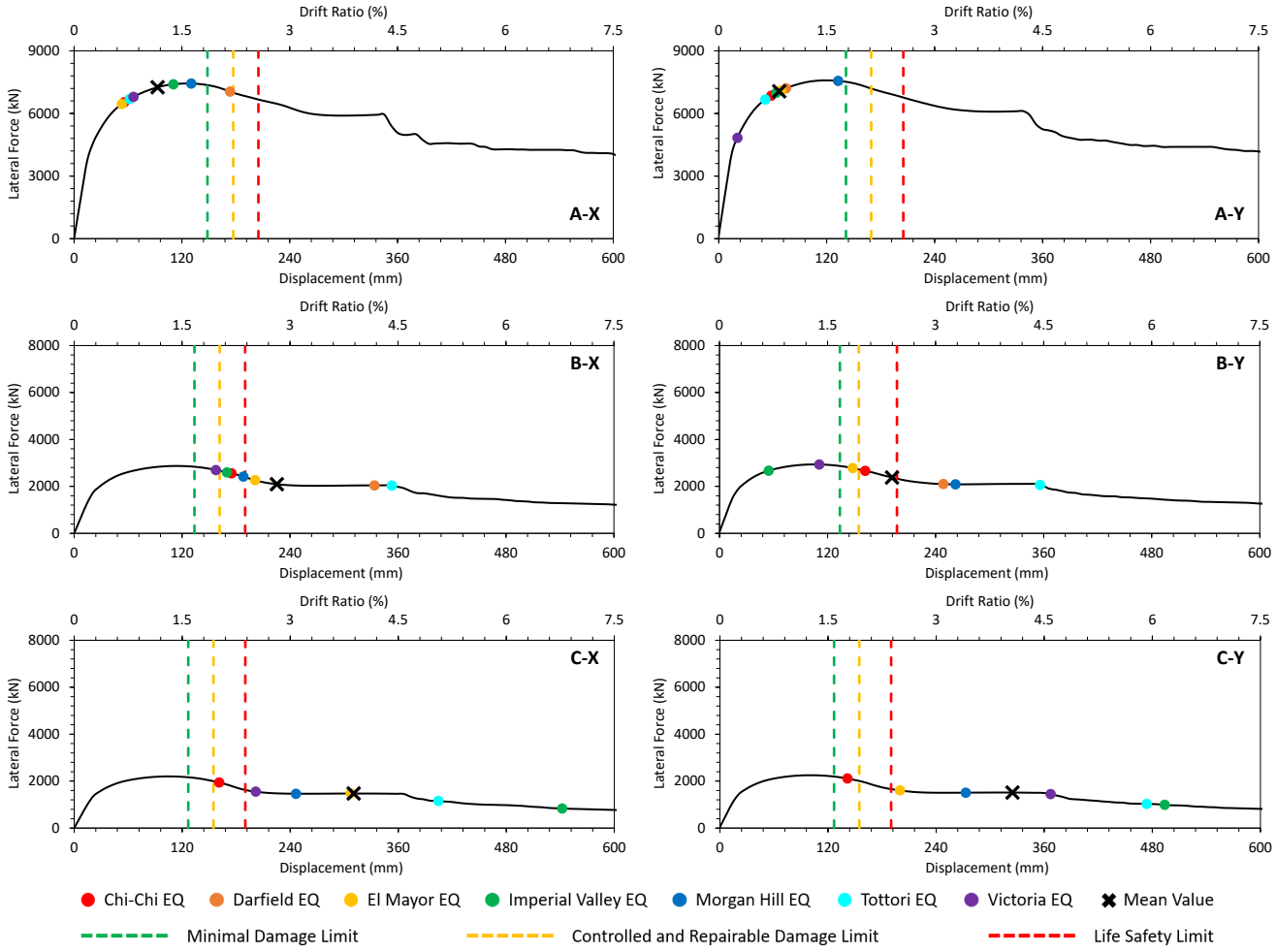

Figure 14 Maximum response in longitudinal (X) and transversal (Y) direction of SOP A, B, and C structures under seismic excitations compared to the corresponding skeleton curves and performance level limits

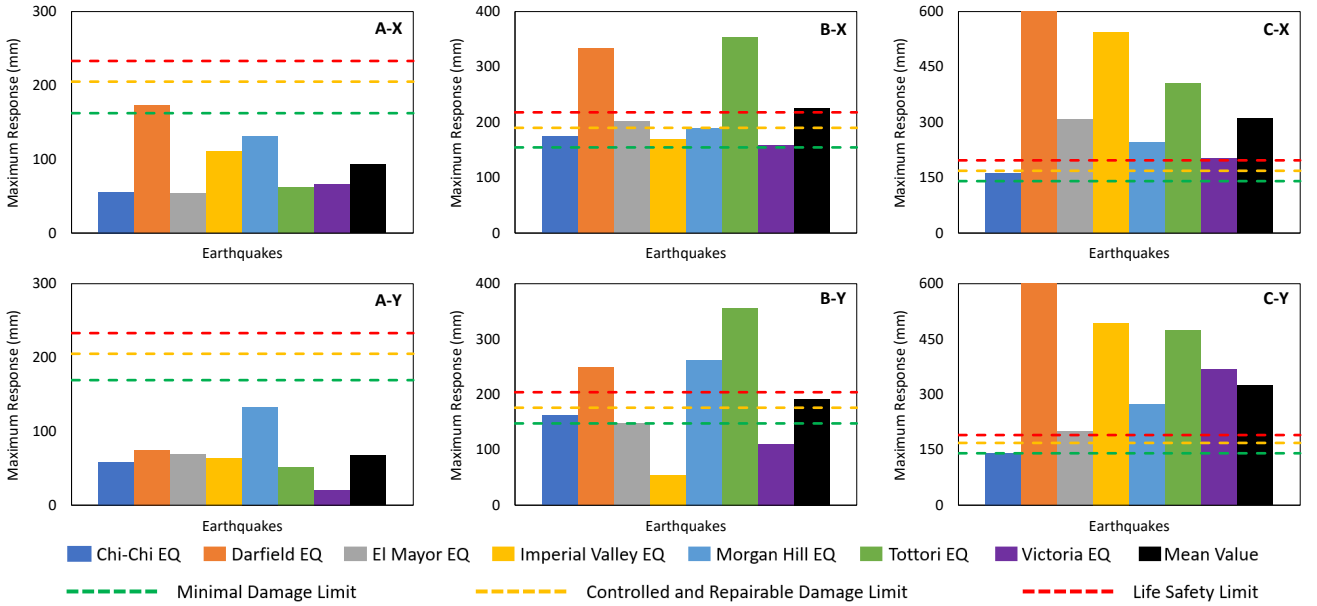

Figure 15 Maximum response in longitudinal (X) and transversal (Y) direction of SOP A, B, and C structures under seismic excitations compared to the performance limit of spun pile concrete material in embedded pile region (Zone B)

4.0 CONCLUSION

Nonlinear pushover and time history analysis were performed to evaluate the response modification factors provided by the Indonesia bridge seismic design code implemented for the SOP structure. Structural behavior and seismic performance of the SOP structures were observed. Some concluding remarks are presented below.

- The response modification factor consideration in the SOP structure's seismic design significantly impacts the demand for pile quantity and structural flexibility. Since implementing a nearly elastic design method, the SOP structure considering an R-value of 1.5 required the most piles. It needed 2.7 and 3.6 times more piles than the SOP structure designed using an *R*-value of 3.5 and 5, respectively. In addition, smaller *R*-values in SOP structure designs result in higher stiffness since more piles are required.
- The nonlinear time history analysis results show that SOP structures exhibit a pinching characteristic. It shows that SOP structures have limited energy dissipation if subjected to seismic excitation. It is consistent with some predecessor study results that spun pile, which is the main component of the SOP structure, has low energy dissipation.
- Spun pile concrete is the material component of an SOP structure most vulnerable to failure, especially under seismic load. So, spun pile concrete governs the performance limit of an SOP structure. However, through careful design of spun pile concrete, there may be an alternative to potentially enhance the seismic performance of the SOP structure.
- As a result of prior failure captured in Zone A, it served as the SOP structure's weak point. Therefore, careful design is required to improve the seismic performance of the SOP structure, particularly in the connection between spun pile and pile head.
- A response modification factor of 1.5 is recommended in the seismic design of an SOP structure since it results in high seismic performance and minimal retrofitting effort after an earthquake occurrence.

Acknowledgment

The authors fully acknowledged to Civil and Engineering Department, Universitas Gadjah Mada, for supporting the computation facility. The authors also thank Prof. Teuku Faisal Fathani, who provided some suggestions for improving the language quality of the paper manuscript.

References

[1] M. Munir and Y. A. Yakin. 2018. Evaluation of Deformation and Stability of Slab Pile Structures on Peat Soil (in Indonesian). *RekaRacana: Jurnal Teknil Sipil.* 4(3) : 105-116. DOI: https://doi.org/10.26760/rekaracana.v4i3.105

[2] G. Benzoni, A. M. Budek, and M. J. N. Priestley. 1997. Experimental Investigation of Ductility of In-Ground Hinges in Solid and Hollow Prestressed Piles. Californina: University of California, San Diego.

[3] Z. Yang, G. Li, W. Wang, and Y. Lv. 2018. Study on the Flexural Performance of Prestressed High Strength Concrete Pile. *KSCE Journal of Civil Engineering.* 22(10) : 4073-4082. DOI: https://doi.org/10.1007/s12205-018-1811-y

[4] A. F. Setiawan, M. F. Darmawan, S. Ismanti, M. Sunarso, and G. M. Adityawarman. 2019. Numerical model for investigating seismic performance of Prestressed Hollow Concrete (PHC) piles with Fiber section element. in *4th International Conference on Earthquake Engineering and Disaster Mitigation*. 1-9.

[5] W. Pawirodikromo. 2012. Engineering Seismology & Earthquake Engineering (in Indonesian) 1st ed. Yogyakarta: Pustaka Pelajar.

[6] M. L. Marsh, I. G. Buckle, R. A. Imbsen, and E. Kavazanjain. 2014. LRFD Seismic Analysis and Design of Bridges. Washington DC: FHWA.

[7] M. Mahmoudi and M. Zaree. 2010. Evaluating response modification factors of concentrically braced steel frames. *Journal of Constructional Steel Research*. 66(10): 1196-1204. DOI: https://doi.org/10.1016/j.jcsr.2010.04.004

[8] D. M. Jasin. 2018. Techncial Design of Pile Slab Bridge (in Indonesian).

[9] D. Putri and T. S. Purwanto. 2018. Design of slab on pile bridge on the Balikpapan Samarinda toll road project segment 1 (in Indoensian). Semarang: Universitas Diponegoro.

[10] ASCE and COPRI. 2014. ACI 61-14 Seismic Design of Piers and Wharves. Virginia: ASCE. Available: www.asce.org/pubs

[11] M. Berliani, Mujiman, and Djuwadi. 2021. Evaluation Experimental of the Dynamic Wharf Structure: A Study Case at Nabire Port, Indonesia. In Proceedings of the 2nd International Seminar of Science and Applied Technology. DOI: https://doi.org/10.2991/aer.k.211106.044

[12] R. R. Foltz, J. M. LaFave, and D. Lee. 2022. Seismic performance of a structural concrete pile-wharf connection before and after retrofit. *Structures*. 38: 874-894. DOI: https://doi.org/10.1016/j.istruc.2022.02.042

[13] L. Su, H. P. Wan, J. Lu, X. Ling, A. Elgamal, and A. K. Arulmoli. 2021. Seismic performance evaluation of a pile-supported wharf system at two seismic hazard levels. *Ocean Engineering*. 219. DOI: https://doi.org/10.1016/j.oceaneng.2020.108333

[14] L. Su et al. 2019. Seismic fragility analysis of pile-supported wharves with the influence of soil permeability. *Soil Dynamics and Earthquake Engineering*. 122: 211-227. DOI: https://doi.org/10.1016/j.soildyn.2019.04.003

[15] L. Su et al. 2020. Seismic performance assessment of a pile-supported wharf retrofitted with different slope strengthening strategies. *Soil Dynamics and Earthquake Engineering*. 129. DOI: https://doi.org/10.1016/j.soildyn.2019.105903

[16] M. Souri, A. Khosravifar, S. Dickenson, N. McCullough, and S. Schlechter. 2023. Numerical modeling of a pile-supported wharf subjected to liquefaction-induced lateral ground deformations. *Computers and Geotechnics*. 154. DOI: https://doi.org/10.1016/j.compgeo.2022.105117

[17] L. Su, H. P. Wan, J. Lu, X. Ling, A. Elgamal, and A. K. Arulmoli. 2021. Seismic performance evaluation of a pile-supported wharf system at two seismic hazard levels. *Ocean Engineering*. 219. DOI: https://doi.org/10.1016/j.oceaneng.2020.108333

[18] S. M. Oktavina, H. A. Shiddiq, R. M. Hutabarat, J. Ramli, and D. I. Imran. 2022. Performance Analysis of Slab on Pile Bridge in Special Soil in Semarang using Nonlinear Static Procedure (in Indonesian). *In HAKI Annual Seminar.*

[19] M.F. Darmawan. 2022. Seismic Performance Investigation of Pile Supported Slab Viaduct Structure Braced With Shear Panel Damper. Master Thesis. Yogyakarta: Universitas Gadjah Mada

[20] Y. Haroki, A. Awaludin, H. Priyosulistyo, A. F. Setiawan, and I. Satyarno. 2023. Seismic Performance Comparison of Simply Supported Hollow Slab on Pile Group Structure with Different Operational Category and Shear Panel Damper Application. *Civil Engineering Dimension*. 25(1): 10-19. DOI: https://doi.org/10.9744/ced.25.1.10-19

[21] C. Irawan, R. Djamaluddin, I. G. P. Raka, and P. Suprobo. 2018. Confinement Behavior of Spun Pile using Low Amount of Spiral Reinforcement - an Experimental Study. *International Journal on Advanced Science Engineering Information Technology*. 8. DOI: https://doi.org/10.18517/ijaseit.8.2.4343

[22] M. T. Davisson and K. E. Robinson. 1965. Bending and Buckling of Partially Embedded Piles. In *Proceedings of the 6th International Conference of ISSMGE*. 243-246.

[23] BSNI. 2016. SNI 2833:2016 Indonesia Seismic Design Bridge Code (in Indonesian). Jakarta: BSN.

[24] FEMA. NEHRP Recommended seismic provisions for new buildings and other structures. *Building Seismic Safety Council*. 2:388.

[25] B. Sunardi. 2015. Synthetic Ground Acceleration in Yogyakarta City Based on Earthquake Hazard Deaggregation. *Jurnal Lingkungan dan Bencana Geologi*. 6 : 211-228.

[26] BSNI. 2020. SNI 8899:2020 Procedures for ground motion selection and modification earthquake resistant buildings design (in Indonesian). Jakarta: BSN.

[27] S. Mazzoni, F. McKenna, M. H. Scott, and G. L. Fenves. 2006. OpenSees command language manual. California: University of California, Berkeley.

[28] ASDEA. 2021. User Manual - Scientific Toolkit for OpenSees. Pescara: ASDEA.

[29] M. F. Darmawan, A. S. Fajar, I. Satyarno, A. Awaludin, and B. A. Yogatama. 2022. Seismic Performance Comparison of Pile Supported Slab Viaduct with PHC Pile and RC Bored Pile in South Part of Java Island. In *Lecture Notes in Civil Engineering, Springer*. 719-734. DOI: https://doi.org/10.1007/978-981-16-7924-7_47